Article

Immunity

Ubiquitin Ligase TRIM62 Regulates CARD9-Mediated Anti-fungal Immunity and Intestinal Inflammation

Graphical Abstract

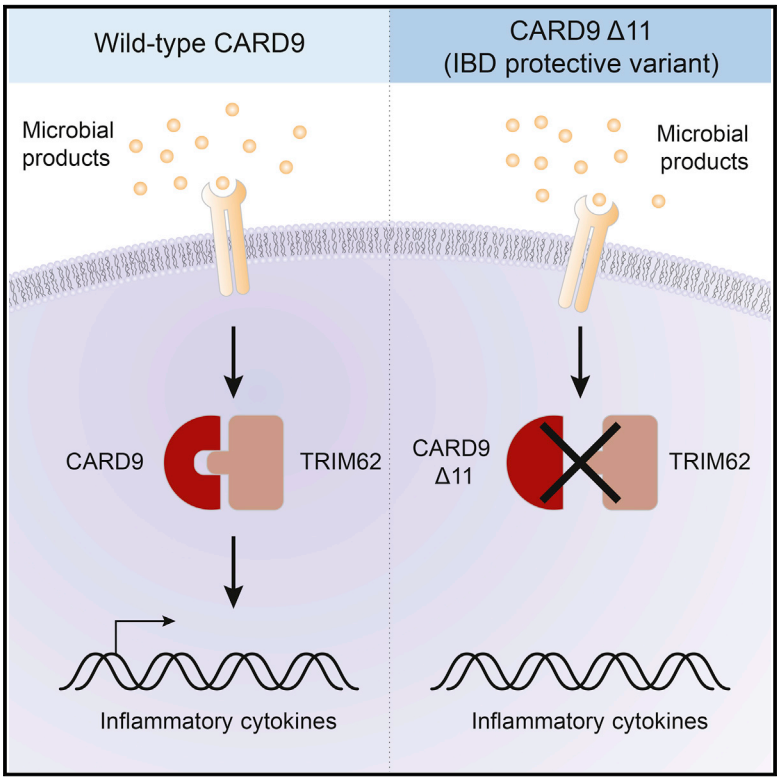

Authors

Zhifang Cao, Kara L. Conway, Robert J. Heath, ..., Terry K. Means, Mark J. Daly, Ramnik J. Xavier

Correspondence

xavier@molbio.mgh.harvard.edu

In Brief

CARD9 is a central component of anti-fungal innate immune signaling, and several immune-related disorders are associated with CARD9 alterations. Cao and colleagues demonstrate an important role for the C terminus in CARD9 signaling and show that ubiquitination of CARD9 by TRIM62 regulates CARD9-mediated anti-fungal immunity.

Highlights

- A *CARD9* allele that protects against disease acts in a dominant-negative manner
- TRIM62-mediated ubiquitination of CARD9 is essential for CARD9 activation
- Ubiquitination by TRIM62 does not occur in a protective variant of CARD9
- *Trim62*-deficient mice show increased susceptibility to fungal infection

Cao et al., 2015, Immunity *43*, 715–726
October 20, 2015 ©2015 Elsevier Inc.
http://dx.doi.org/10.1016/j.immuni.2015.10.005

Immunity
Article

Ubiquitin Ligase TRIM62 Regulates CARD9-Mediated Anti-fungal Immunity and Intestinal Inflammation

Zhifang Cao,[1,2] Kara L. Conway,[1,2,3] Robert J. Heath,[1,2,3] Jason S. Rush,[3] Elizaveta S. Leshchiner,[3] Zaida G. Ramirez-Ortiz,[4] Natalia B. Nedelsky,[1,2] Hailiang Huang,[3,5] Aylwin Ng,[1,2,3] Agnès Gardet,[1,2] Shih-Chin Cheng,[6] Alykhan F. Shamji,[3] John D. Rioux,[7] Cisca Wijmenga,[8] Mihai G. Netea,[6] Terry K. Means,[4] Mark J. Daly,[3,5] and Ramnik J. Xavier[1,2,3,*]

[1]Gastrointestinal Unit and Center for the Study of Inflammatory Bowel Disease, Massachusetts General Hospital and Harvard Medical School, Boston, MA 02114, USA
[2]Center for Computational and Integrative Biology, Massachusetts General Hospital and Harvard Medical School, Boston, MA 02114, USA
[3]Broad Institute of MIT and Harvard, Cambridge, MA 02142, USA
[4]Center for Immunology and Inflammatory Diseases and Division of Rheumatology, Allergy, and Immunology, Massachusetts General Hospital and Harvard Medical School, Charlestown, MA 02129, USA
[5]Analytic and Translational Genetics Unit, Massachusetts General Hospital and Harvard Medical School, Boston, MA 02114, USA
[6]Department of Internal Medicine and Radboud Center for Infectious Diseases, Radboud University Nijmegen Medical Center, Nijmegen 6525 GA, the Netherlands
[7]Research Center, Montreal Heart Institute and Université de Montréal, QC H1T 1C8, Canada
[8]Department of Genetics, University Medical Center Groningen, University of Groningen, Groningen T9700 RB, the Netherlands
*Correspondence: xavier@molbio.mgh.harvard.edu
http://dx.doi.org/10.1016/j.immuni.2015.10.005

SUMMARY

CARD9 is a central component of anti-fungal innate immune signaling via C-type lectin receptors, and several immune-related disorders are associated with CARD9 alterations. Here, we used a rare CARD9 variant that confers protection against inflammatory bowel disease as an entry point to investigating CARD9 regulation. We showed that the protective variant of CARD9, which is C-terminally truncated, acted in a dominant-negative manner for CARD9-mediated cytokine production, indicating an important role for the C terminus in CARD9 signaling. We identified TRIM62 as a CARD9 binding partner and showed that TRIM62 facilitated K27-linked poly-ubiquitination of CARD9. We identified K125 as the ubiquitinated residue on CARD9 and demonstrated that this ubiquitination was essential for CARD9 activity. Furthermore, we showed that similar to *Card9*-deficient mice, *Trim62*-deficient mice had increased susceptibility to fungal infection. In this study, we utilized a rare protective allele to uncover a TRIM62-mediated mechanism for regulation of CARD9 activation.

INTRODUCTION

CARD9 is a central adaptor protein in innate immune signaling via C-type lectin receptors (CLRs), such as Dectin-1, Dectin-2, and Mincle (Goodridge et al., 2009; Gross et al., 2006; Ishikawa et al., 2009; Roth and Ruland, 2013; Saijo et al., 2010; Schoenen et al., 2010; Werninghaus et al., 2009), and has more recently been reported to regulate cytokine production induced by cytosolic nucleic acid sensors RIG-I and Rad50 in mouse models (Abdullah et al., 2012; Poeck et al., 2010; Roth et al., 2014). CLRs sense components of fungal and bacterial cell walls, linking signaling from these immune receptors to nuclear factor-κB (NF-κB) activation through a series of sequential phosphorylation events. CARD9 thereby mediates production of pro-inflammatory cytokines, including tumor necrosis factor α (TNFα), interleukin-6 (IL-6), and IL-1β, ultimately regulating the responses of T helper 1 (Th1) and Th17 cells (Drummond et al., 2011; Glocker et al., 2009; LeibundGut-Landmann et al., 2007; Marakalala et al., 2010; Robinson et al., 2009; Saijo et al., 2010; Sokol et al., 2013).

CARD9 was recently identified as a gene associated with determining risk for inflammatory bowel disease (IBD) (Jostins et al., 2012; Rivas et al., 2011), ankylosing spondylitis (Pointon et al., 2010), primary sclerosing cholangitis (Janse et al., 2011), and immunoglobulin A (IgA) nephropathy (Kiryluk et al., 2014). Patients with early stop codons or point mutations affecting the N-terminal portion of CARD9 also show increased susceptibility to fungal infection (Drewniak et al., 2013; Gavino et al., 2014; Gazendam et al., 2014; Glocker et al., 2009; Grumach et al., 2015; Herbst et al., 2015; Jachiet et al., 2015; Lanternier et al., 2015a; Lanternier et al., 2015b; Lanternier et al., 2013; Wang et al., 2014). Unlike most genetic risk factors for complex diseases, *CARD9* alleles exist in both predisposing and protective forms for IBD. The predisposing variant, CARD9 S12N, is caused by a common coding SNP that was identified via genome-wide association studies (GWASs) and is associated with increased expression of *CARD9* mRNA (Franke et al., 2010; Jostins et al., 2012; McGovern et al., 2010; Zhernakova et al., 2008). The protective variant, CARD9 S12NΔ11, is caused by a rare splice variant in which exon 11 of *CARD9* is deleted. This allele, identified by deep sequencing of GWAS loci, results in a protein with a C-terminal truncation and confers strong protection against disease ($p < 10^{-16}$) (Beaudoin et al., 2013; Rivas et al., 2011).

The CARD9 signaling cascade is initiated after engagement of Dectin-1 by β-glucans (which results in the phosphorylation of Dectin-1 itself) or engagement of Dectin-2 or Mincle by fungal mannans (which results in phosphorylation of the ITAM-containing signaling adaptor FcRγ). These phosphorylation events activate Syk kinase, which subsequently activates PKCδ to phosphorylate CARD9 at T231 (Strasser et al., 2012). Phosphorylated CARD9 recruits BCL10 and MALT1 to form a CARD9-BCL10-MALT1 (CBM) complex, which activates the canonical NF-κB pathway (Roth and Ruland, 2013). Rubicon acts as a feedback inhibitor by displacing CARD9 from the CBM complex and thereby terminating CARD9-mediated signaling (Yang et al., 2012). Interestingly, a recent report showed that Dectin-1-CARD9 signaling induces neutrophilic myeloid-derived suppressor cells; these cells functionally suppress T and natural killer (NK) cell responses, suggesting that the CARD9 pathway might play an important role in balancing inflammation in response to pathogenic fungi (Rieber et al., 2015).

Aside from the kinase-dependent steps that contribute to the initiation of the CBM signalosome and Rubicon-dependent feedback inhibition, little is known regarding other mechanisms that might regulate the assembly, stability, or activity of CARD9 in this complex. CARD9 is a scaffold protein with an N-terminal domain composed of a CARD domain followed by two coiled-coil domains. However, CARD9 has no clear domain within its C terminus, and its mode of regulation is not fully defined (Hara and Saito, 2009; Roth and Ruland, 2013).

In this study, we used disease-associated *CARD9* alleles to uncover fundamental insights into the protein-protein interactions and post-translational modifications that regulate CARD9 function. We demonstrated that the C terminus of CARD9 is a critical regulatory module for CARD9 activity and identified TRIM62 as a novel interactor with the CARD9 C terminus. We showed that TRIM62 ubiquitinates CARD9 at K125 and demonstrated that a CARD9 alteration at this residue (K125R) abrogates CLR-induced CARD9-mediated cytokine production. Furthermore, *Trim62*$^{-/-}$ mice showed reduced CLR-CARD9-dependent cytokine production and increased susceptibility to fungal infection. In parallel, we showed that the protective CARD9 Δ11 variant acts in a dominant-negative fashion for CLR-CARD9-dependent cytokine signaling and that TRIM62-mediated ubiquitination does not occur in this variant protein.

RESULTS

The C Terminus of CARD9 Is Essential for CARD9 Activation

The association between IBD and CARD9, which has both protective and predisposing alleles, raises the need to characterize regulatory mechanisms for CARD9-dependent pathways. To this end, we employed naturally occurring CARD9 variants characterized by C-terminal truncations to investigate CARD9 regulation. We first used a human immune cDNA panel to collect a library of naturally occurring human *CARD9* alleles and screened this collection for effects on CARD9-mediated cytokine production. In addition to identifying full-length CARD9 and the disease-associated S12N and S12NΔ11 alleles, we also identified several novel variants of CARD9 (Figures 1A and S1A) and noted that the majority of the allelic variations affected the C-terminal portion of the protein.

To definitively evaluate whether the deletion of exon 11 (Δ11) imparts protection from disease, we analyzed Immunochip datasets with 33,311 IBD-affected individuals and 33,938 healthy control individuals from the International Inflammatory Bowel Disease Genetics Consortium (IIBDGC) and found that individuals with the Δ11 splice variant are less likely to develop IBD regardless of the presence of S12N alteration (Figure S1B), further suggesting an important functional role for the C terminus of CARD9.

To examine how C-terminal truncation affects CARD9 function, we stimulated CARD9-dependent pathways by using either depleted zymosan, a glucan-enriched preparation that is derived from fungal cell walls and mainly activates Dectin-1 (Gross et al., 2006), or trehalose 6,6-dimycolate (TDM), a mycobacterial cell-wall component that activates two other CLRs: Mincle and macrophage C-type lectin (Miyake et al., 2013; Roth and Ruland, 2013; Werninghaus et al., 2009). Activation by these two ligands led to CARD9-dependent production of proinflammatory cytokines, including TNFα and IL-6 (Figure S1C) (Gross et al., 2006; Saijo et al., 2010; Werninghaus et al., 2009). We therefore re-expressed human CARD9 isoforms in murine *Card9*$^{-/-}$ bone-marrow-derived dendritic cells (BMDCs) and assessed cytokine production in response to these ligands by ELISA (Figures 1B–1E and S1D–S1F). BMDCs expressing the predisposing variant CARD9 S12N showed greater TNFα and IL-6 production than BMDCs expressing wild-type CARD9. In contrast, CARD9 Δ11 and CARD9 S12NΔ11, as well as the C-terminally truncated CARD9 V6, showed significant impairment in TNFα and IL-6 production. This effect did not occur when cytokine production was stimulated by lipopolysaccharide (LPS), a ligand for Toll-like receptor 4 (TLR4), indicating that the impairment was specific to the CARD9 pathway (Figures 1D and S1E). These data suggest that the C terminus of CARD9 is required for CLR-CARD9-mediated cytokine production.

A Protective CARD9 Variant Acts in a Dominant-Negative Manner

Pursuing our finding that CARD9 Δ11 demonstrates loss of CARD9 function (Figure 1), we next examined whether this variant would have a dominant-negative effect on CARD9 function when co-expressed with wild-type CARD9 in human cells. To test this hypothesis, we expressed CARD9 Δ11 in the human monocytic cell line THP-1, as well as in primary human monocyte-derived dendritic cells (MDDCs), and found that CARD9 Δ11 suppressed depleted zymosan-induced NF-κB activation in THP-1 cells (Figures 2A and 2B) and depleted zymosan-induced TNFα production in MDDCs (Figures S2A and S2B). Consistent with these findings, we also expressed CARD9 Δ11 in wild-type murine BMDCs and found that CARD9 Δ11 inhibited TDM-induced TNFα and IL-6 production (Figures S2C and S2D). In contrast, LPS-induced cytokine production was unaltered under the same experimental conditions in both human MDDCs and murine BMDCs (Figures S2E and S2F). Collectively, the results indicate that CARD9 Δ11 has a dominant-negative effect in both human and mouse dendritic cells. Furthermore, FLAG-tagged human CARD9 Δ11 co-immunoprecipitated with endogenous CARD9 in wild-type murine BMDCs (Figure 2C). This

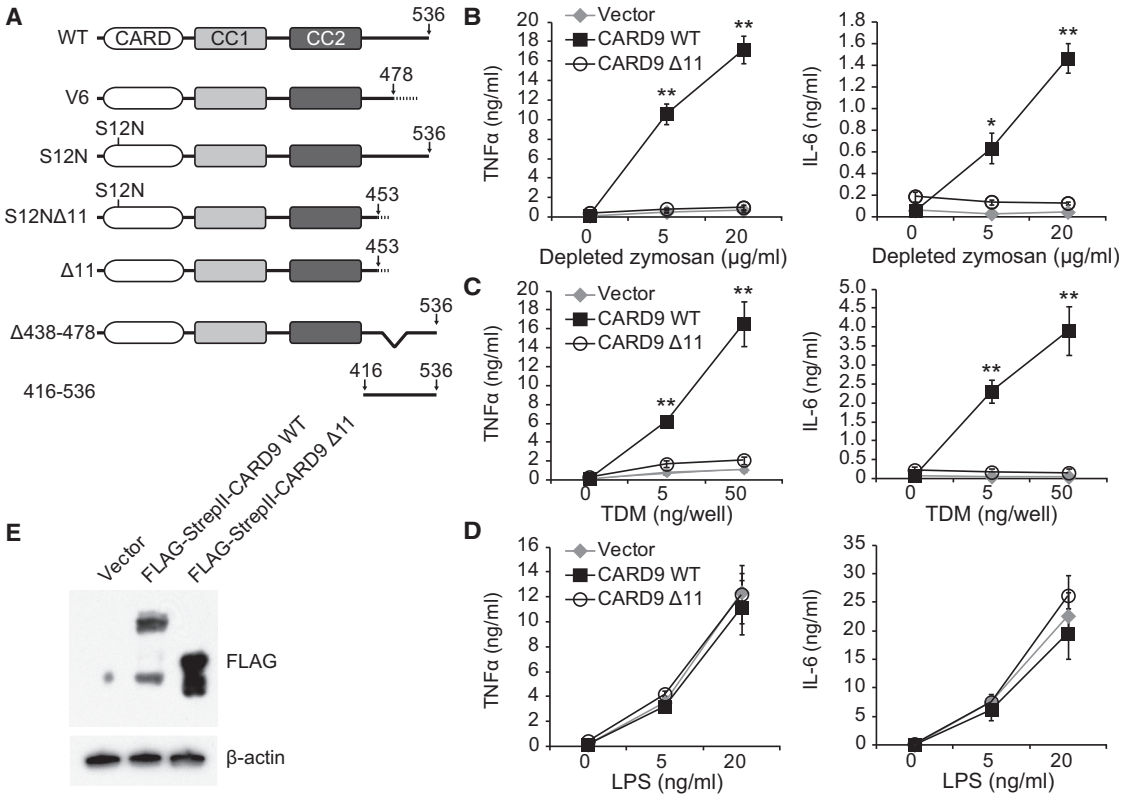

Figure 1. C-Terminal CARD9 Truncations Impair Depleted Zymosan- and TDM-Induced Cytokine Production

(A) Schematic of CARD9 variants used. All indicated variants, with the exception of CARD9 416–536 (which was designed for experimental use), were found in a human immune cDNA panel. CC, coiled-coil domain.

(B–D) *Card9*$^{-/-}$ murine BMDCs transduced with the indicated CARD9 variants were stimulated with depleted zymosan, TDM, or LPS, and cytokine amounts were assessed by ELISA. Data were obtained from three independent experiments performed in duplicate (n = 3 mice per experiment).

(E) Expression of CARD9 variants in total lysates from (B)–(D) as detected by western blot. Bars represent means ± SD. *$p < 0.05$, **$p < 0.01$. Comparisons in (B)–(D) are relative to stimulated wild-type (WT) CARD9.

See also Figure S1.

result demonstrates that CARD9 Δ11 can form a complex with endogenous full-length CARD9, suggesting that CARD9 Δ11 might inhibit CARD9 function via hetero-oligomerization with full-length CARD9. To pursue these findings, we developed an ELISA-based assay that detects the interaction between differentially tagged purified CARD9 proteins in vitro in a cell-free system. By using GST- and FLAG-tagged purified CARD9 constructs, we confirmed that both wild-type CARD9 and CARD9 Δ11 are capable of directly interacting with CARD9. Importantly, the ability of CARD9 Δ11 to form complexes with wild-type CARD9 was not impaired (Figure 2D).

TRIM62 Binds the C Terminus of CARD9

Because CARD9 functions as a scaffold protein, we next investigated whether loss of specific protein-protein interactions by C-terminally truncated proteins might underlie their effects on CARD9 function. Because the details of how the C terminus of CARD9 delivers signals from receptors to effectors are largely unknown, we sought to identify novel CARD9 binding partners that might be responsible for the loss of signal transduction in the truncated proteins. To this end, we re-expressed a tagged version of wild-type CARD9 in immortalized *Card9*$^{-/-}$ cells (Blasi et al., 1985) and employed tandem affinity purification to purify CARD9. Using mass spectrometry, we identified TRIM62 as a top hit co-purified with CARD9 on the basis of high peptide counts and a high percentage of protein coverage.

Members of the TRIM family of proteins are involved in multiple cellular processes, including innate immunity (Uchil et al., 2013; Versteeg et al., 2013), and mutations in multiple TRIM-encoding genes are associated with human disease (Marín, 2012; McNab et al., 2011). However, most studies of TRIM proteins have employed overexpression or knockdown approaches (Arimoto et al., 2010; Tsuchida et al., 2010; Uchil et al., 2013; Versteeg et al., 2013), and very few studies in knockout mice or human cells have examined ligand specificity (Gack et al., 2007; Zhang et al., 2013). We next examined whether we could detect a direct interaction between CARD9 and TRIM62. To demonstrate TRIM62 binding of CARD9, we developed an ELISA-based system that employs differentially tagged CARD9 and TRIM62. These experiments demonstrated that wild-type CARD9, but not CARD9 Δ11, interacted with TRIM62, as assessed by CARD9-TRIM62 ELISA. Addition of purified C-terminal domain (CTD) of CARD9 abrogated this interaction, supporting the hypothesis that TRIM62 binds the C terminus of CARD9

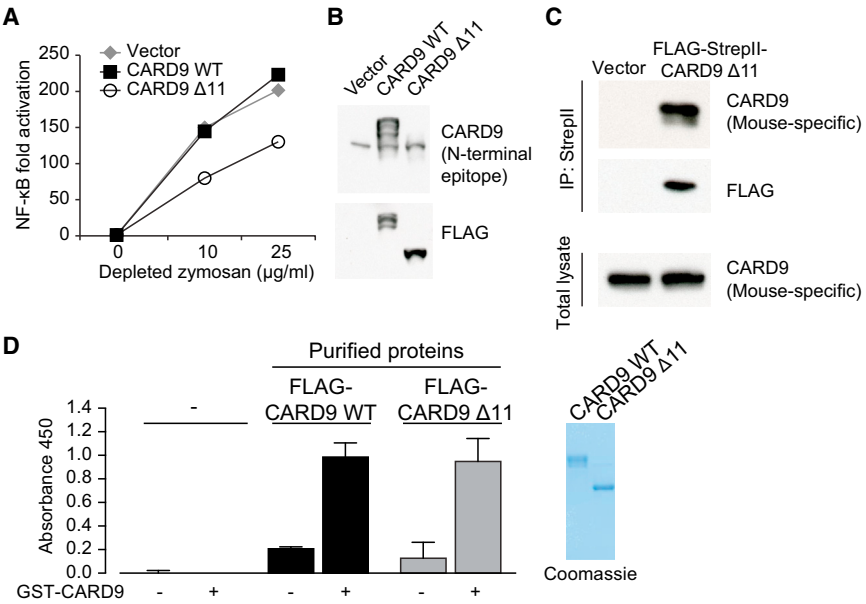

Figure 2. CARD9 Δ11 Is a Dominant-Negative Variant

(A) THP-1 cells were transduced with wild-type (WT) FLAG-CARD9 or FLAG-CARD9 Δ11 and stimulated with depleted zymosan. NF-κB amounts were assessed by NF-κB luciferase assay.

(B) A western blot shows expression of CARD9 as detected by antibodies against endogenous CARD9 (top) or FLAG (bottom) in lysates from (A). Note that the antibody detecting endogenous CARD9 has an N-terminal epitope and therefore does not recognize CARD9 Δ11.

(C) WT BMDCs were transduced with FLAG-StrepII empty vector or FLAG-StrepII-tagged CARD9Δ11 and then immunoprecipitated for tagged CARD9 Δ11.

(D) Purified FLAG-tagged WT CARD9 and CARD9 Δ11 were incubated with immobilized GST-CARD9; interactions were assessed by ELISA. Coomassie gel on the right shows purified proteins used in the ELISA.

See also Figure S2.

(Figure S3A). To further study the molecular interaction between CARD9 and TRIM62 and the dominant-negative effect of CARD9 Δ11, we developed a cell-based BRET (bioluminescence resonance energy transfer) system that enables detection of specific protein-protein interactions in the context of an intact cell. BRET has been used for characterizing disease-related genetic variants of GNAL (Fuchs et al., 2013), as well as for investigating the function of cancer-associated PTEN alterations in a dominant-negative context (Papa et al., 2014). Notably, a BRET assay was recently used for discovering a novel CARD9 interactor in a physiologic setting (Roth et al., 2014). In our BRET system, nanoluciferase-tagged CARD9 (donor) can interact with Halo-tagged TRIM62 (acceptor) to generate energy measured as a BRET signal (Figure S3B). We first confirmed that the assay robustly detects an interaction between CARD9 and TRIM62. In agreement with our findings that the interaction is mediated by the C terminus of CARD9, we found that the interaction can be competitively disrupted by co-expression of the CARD9 C terminus (amino acids 416–536) (Figure S3C). To more precisely examine the dominant-negative effect of CARD9 Δ11, we assessed the interaction between CARD9 and TRIM62 in the presence of co-expressed CARD9 Δ11 or negative controls such as unrelated proteins SULT1 and LacZ (Figure S3D). The presence of CARD9 Δ11 disrupted the CARD9-TRIM62 interaction, whereas SULT1, LacZ, or vector alone showed no effect. These results demonstrate the inhibitory effect of the protective variant on the CARD9-TRIM62 interaction and support the hypothesis that hetero-oligomerization of wild-type CARD9 and CARD9 Δ11 might functionally inhibit signaling of wild-type CARD9.

Consistent with these findings, co-immunoprecipitation studies of CARD9 and TRIM62 demonstrated that CARD9 Δ11, CARD9 S12NΔ11, and CARD9 V6 failed to bind TRIM62, whereas the CARD9 C terminus alone (amino acids 416–536) bound TRIM62 even more efficiently than full-length wild-type CARD9 (Figure 3A). We further confirmed these results by demonstrating that endogenous CARD9 interacted with endogenous TRIM62 in a zymosan-dependent manner in THP-1 cells (Figure S3E). These results demonstrate that these proteins interact endogenously in an activation-dependent manner.

Having found a biochemical interaction between TRIM62 and CARD9, we next examined their colocalization by immunofluorescence. We found that TRIM62 co-localized with wild-type CARD9 and CARD9 S12N but did not co-localize with CARD9 variants lacking the C terminus (CARD9 Δ11, CARD9 S12N Δ11, or CARD9 V6) in HeLa cells (Figures S3F–S3H); all isoforms of CARD9 showed relatively diffuse cytoplasmic localization when expressed alone, whereas TRIM62 showed a diffuse localization with some cytoplasmic bodies, consistent with localization patterns observed for TRIM5α (Campbell et al., 2007) and TRIM22 (Reymond et al., 2001) (Figures S3F–S3H). Consistent with these observations, endogenous CARD9 and TRIM62 co-localized in a zymosan-dependent manner in wild-type BMDCs (Figures 3B and 3C).

Furthermore, using THP-1 cells in which endogenous *CARD9* had been deleted with CRISPR, we re-expressed tagged wild-type CARD9 or CARD9 Δ11 and found that although wild-type CARD9 colocalized with endogenous TRIM62 in a stimulation-dependent manner, CARD9 Δ11 did not (Figures 3D and 3E). Notably, TRIM62 co-localized with BCL10, a well-characterized CARD9 interactor, in a zymosan-dependent manner in wild-type BMDCs, suggesting that TRIM62 might associate with CARD9 as part of the CBM complex (Figures S3I and S3J).

TRIM62 Induces K27-Linked CARD9 Ubiquitination

We next examined the functional consequences of the CARD9-TRIM62 interaction. TRIM family proteins generally modify their targets via E3 ligase activity, which can include ubiquitination, SUMOylation, or ISGylation (Chu and Yang, 2011; McNab et al., 2011). We found that TRIM62 specifically promoted CARD9 ubiquitination in HEK293T cells (Figure 4A) and confirmed that endogenous CARD9 was ubiquitinated in a

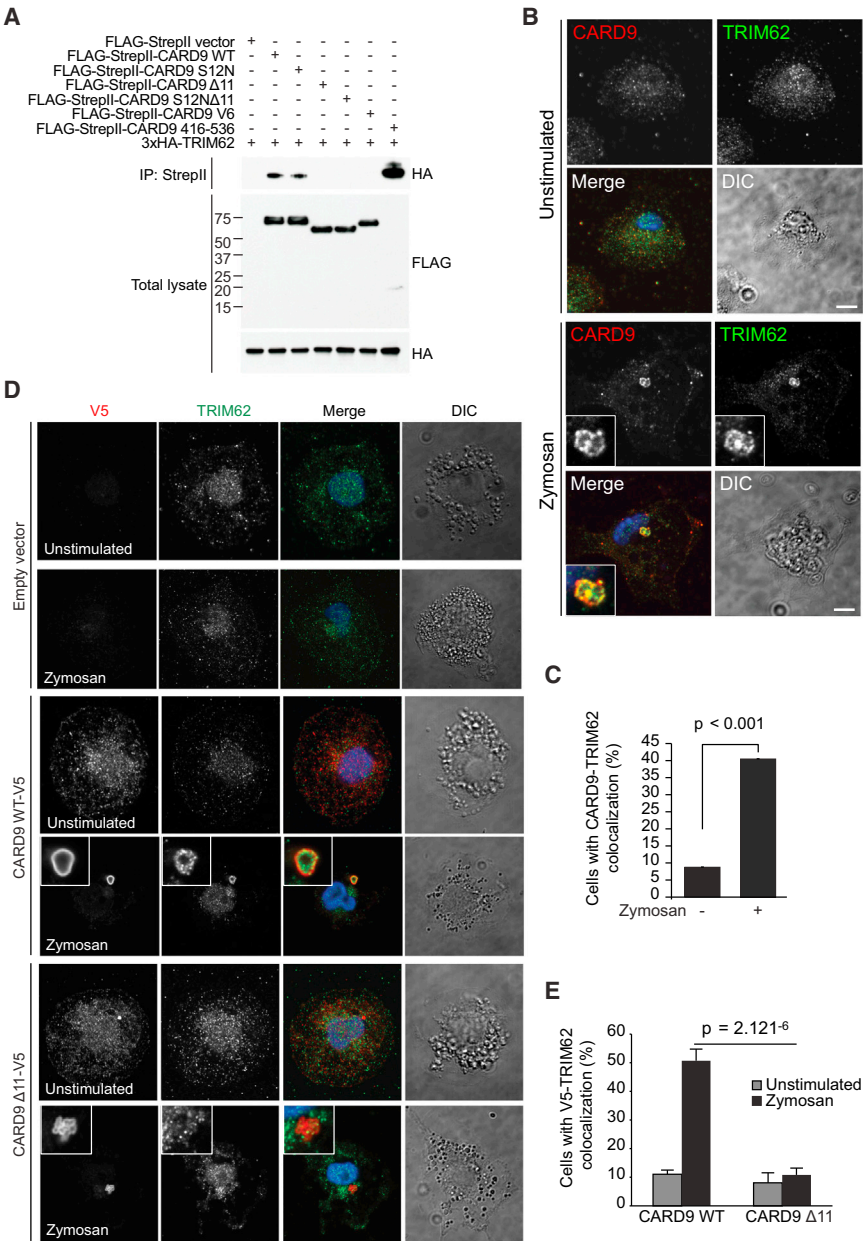

Figure 3. TRIM62 Interacts with Full-Length CARD9, but Not CARD9 C-Terminal Truncations

(A) HEK293T cells were transfected with the indicated constructs and then immunoprecipitated for tagged CARD9.

(B) Wild-type (WT) BMDCs were stimulated with depleted zymosan and stained for endogenous CARD9 and TRIM62. Scale bars represent 5 μm.

(C) Quantification of results shown in (B).

(D) *CARD9*$^{-/-}$ THP-1 cells were transduced with V5-tagged WT CARD9 or CARD9 Δ11 and stimulated with depleted zymosan. Cells were stained for endogenous TRIM62 and tagged CARD9.

(E) Quantification of results shown in (D).

See also Figure S3.

stimulation-dependent manner in dendritic cells (Figure 4B). We next designed an E3-ligase-dead variant of TRIM62 by changing two conserved catalytic cysteines in the RING domain to alanine (TRIM62 C11A;C14A) (Deshaies and Joazeiro, 2009) and showed that CARD9 ubiquitination was dependent on E3 ligase activity in HEK293T cells (Figure 4C). Importantly, CARD9 Δ11 was not ubiquitinated by TRIM62 (Figure 4D). Similarly to wild-type TRIM62, TRIM62 C11A;C14A colocalized extensively with CARD9 (Figure S4).

Next, we identified which type of ubiquitin linkage was occurring on CARD9 and showed that ubiquitination was dramatically reduced by a K27R alteration in ubiquitin (Figure 4E). In a reciprocal assay using ubiquitin mutants that each contained only one lysine, we found that K27 alone was sufficient for TRIM62-mediated ubiquitination of CARD9 (Figure 4F). Altogether, we conclude that TRIM62 mediates K27-linked ubiquitination of full-length CARD9, but not CARD9 Δ11.

CARD9 Ubiquitination by TRIM62 Plays a Critical Role in CLR-CARD9 Signaling

To identify the specific CARD9 lysine target or targets ubiquitinated by TRIM62, we first examined all 40 lysines in human CARD9. We identified 17 of these lysines as being absolutely conserved across 17 mammalian species and elected to individually change each of these residues to arginine. We found that alteration of K125 significantly reduced TRIM62-mediated CARD9 poly-ubiquitination in HEK293T cells (Figure 5A). Importantly, using in vitro ubiquitination assays with purified proteins, we verified that CARD9 was directly ubiquitinated by TRIM62 at residue K125; this ubiquitination was dependent on the ligase activity of TRIM62 and did not occur in CARD9 Δ11 (Figure 5B).

To identify the functional consequence of this ubiquitination, we re-expressed this ubiquitination-deficient CARD9 in *Card9*$^{-/-}$ BMDCs. We found that K125R abolished CARD9-mediated cytokine production upon depleted zymosan or TDM stimulation (Figures S5A–S5D), indicating that ubiquitination of CARD9 K125 is critical for CARD9 activation. Similar results were obtained in human *CARD9*$^{-/-}$ THP-1 cells reconstituted with wild-type CARD9 or CARD9 K125R. In this system, we found that stimulation-dependent NF-κB activity was dramatically reduced by the introduction of K125R (Figures 5C and 5D). Notably, in *Card9*$^{-/-}$ BMDCs reconstituted with wild-type CARD9 or CARD9 K125R, both the wild-type and altered forms of CARD9 retained zymosan-dependent colocalization with BCL10 (Figures S5E and S5F). However, the CARD9-BCL10 interaction remained unproductive in the context of K125R, as shown by the disruption of NF-κB activity by this alteration. Taken together, these results demonstrate

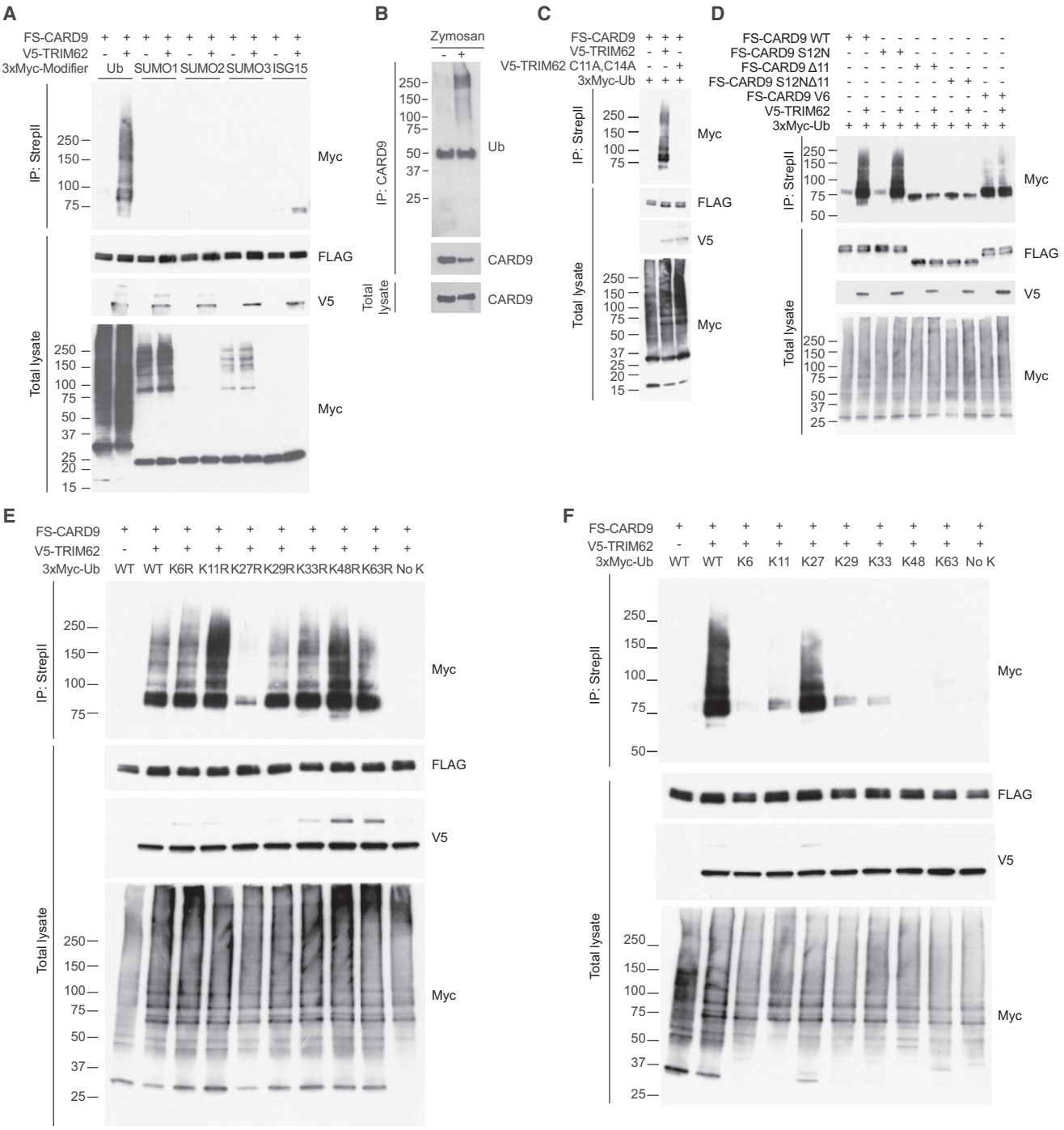

Figure 4. TRIM62 Promotes the Ubiquitination of Full-Length CARD9, but Not CARD9 Truncations

(A) HEK293T cells were transfected with indicated constructs, immunoprecipitated for tagged CARD9, and then blotted for tagged ubiquitin, SUMO1, SUMO2, SUMO3, and ISG15.

(B) Wild-type (WT) BMDCs were stimulated with depleted zymosan, immunoprecipitated for CARD9, and then blotted for endogenous CARD9 and ubiquitin.

(C) HEK293T cells were transfected with indicated constructs, immunoprecipitated for tagged CARD9, and then blotted for ubiquitin in the presence of either WT or a ligase-dead (C11A;C14A) version of TRIM62.

(D) HEK293T cells were transfected with indicated constructs, immunoprecipitated for tagged CARD9, and then blotted for tagged ubiquitin.

(E and F) HEK293T cells were transfected with indicated constructs, immunoprecipitated for tagged CARD9, and then blotted for indicated ubiquitin mutants. In (E), transfected ubiquitin constructs have single point alterations in the indicated lysine residues. In (F), transfected ubiquitin constructs have point alterations in multiple lysines, leaving only the indicated lysine residue intact. FS, FLAG-StrepII.

See also Figure S4.

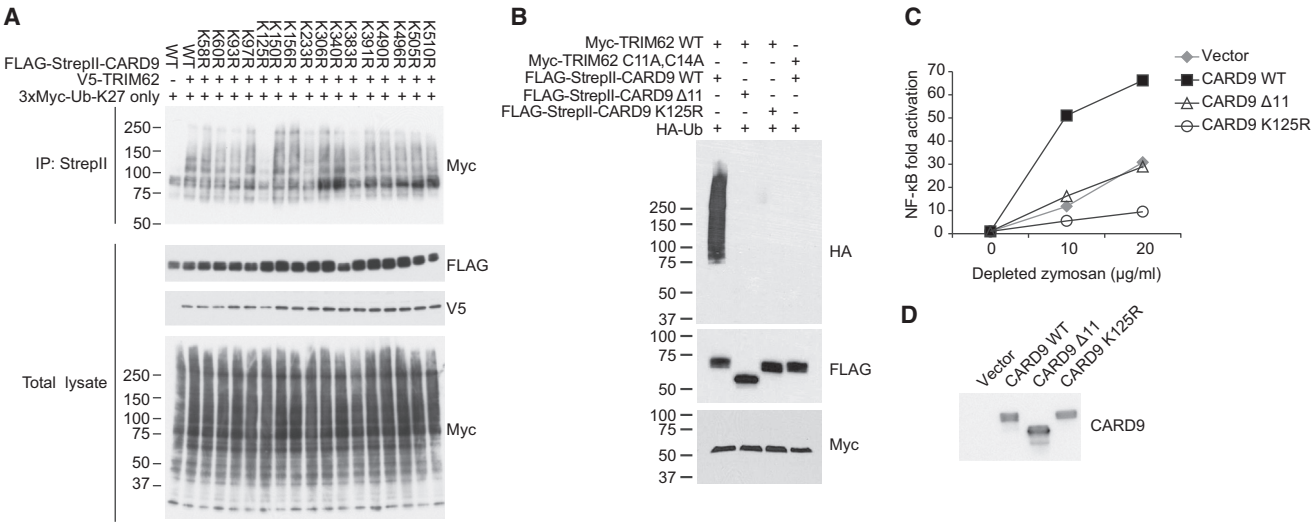

Figure 5. TRIM62-Mediated CARD9 Ubiquitination at K125 Is Critical for CARD9 Activation

(A) HEK293T cells were transfected with TRIM62, ubiquitin (K27 only), and CARD9 with the indicated point alterations and then immunoprecipitated for CARD9.

(B) The indicated proteins were purified and incubated in vitro for assessing ubiquitination of CARD9.

(C) *CARD9*$^{-/-}$ THP-1 cells were reconstituted with wild-type (WT) CARD9, CARD9 Δ11, or CARD9 K125R and stimulated with depleted zymosan, and NF-κB amounts were assessed by NF-κB luciferase assay.

(D) A western blot shows expression levels of CARD9 in the cells used in (C).

See also Figure S5.

that K125-mediated ubiquitination is critical for CARD9-mediated NF-κB signaling.

TRIM62 Regulates Immune Responses and Susceptibility to *Candida albicans* Infection In Vivo

To directly assess whether the novel CARD9 interactor TRIM62 is important for immune responses elicited via the CARD9 signaling pathway, we generated *Trim62*$^{-/-}$ mice (Figures S6A and S6B). Intravenous injection of heat-killed *C. albicans*, a fungal pathogen that activates the CLR-CARD9 pathway, induced acute, systemic IL-6 production, which was significantly impaired in the absence of TRIM62 (Figure 6A).

To examine pathways involved in pro-inflammatory cytokine production, we used intracellular staining and flow cytometry to measure activity of both NF-κB and mitogen-activated protein kinase (MAPK) pathways, given that a recent study in macrophages identified a role for ERK signaling in susceptibility to *Candida* (Jia et al., 2014). Isolated wild-type and *Trim62*$^{-/-}$ splenic dendritic cells were stimulated ex vivo for 10 min with LPS or heat-killed *C. albicans*. Consistent with the in vivo findings, *Trim62*$^{-/-}$ dendritic cells had less phosphorylated IκBα and ERK1/2 in response to heat-killed *C. albicans* stimulation, indicating impaired NF-κB and MAPK signaling, respectively (Figure S6C). This difference was not observed in response to LPS, indicating that the impaired signaling was specific to the CLR-CARD9 signaling pathway. These results are in agreement with a recent report showing that *TRIM62* knockdown in human primary macrophages did not affect MyD88-dependent signaling at early time points (Uchil et al., 2013).

In addition to observing impaired proinflammatory pathway activation and cytokine production in response to heat-killed *C. albicans*, we found by using live *C. albicans* infection that *Trim62*$^{-/-}$ mice had significantly more *C. albicans* colony-forming units (CFUs) present in the kidney, spleen, and liver (Figure 6B), suggesting impaired pathogen clearance. To determine whether the increased fungal burden in *Trim62*$^{-/-}$ mice after in vivo infection was due to defective phagocytosis, we exposed bone-marrow-derived macrophages (BMDMs) to fluorescently labeled *C. albicans* and determined uptake via flow cytometry. Uptake of *C. albicans* was comparable in wild-type and *Trim62*$^{-/-}$ mice, indicating that the enhanced fungal burden in *Trim62*$^{-/-}$ mice was not due to differences in phagocytosis efficiency (Figure 6C). Additionally, expression of cytokines and chemokines important during *C. albicans* infection was significantly lower in *Trim62*$^{-/-}$ mice than in wild-type mice, suggesting that downstream inflammatory signaling events (through the TRIM62-CARD9 pathway) are blunted (Figure S6D). Lastly, to determine whether the decreased cytokine responses and increased fungal burden in *Trim62*$^{-/-}$ mice after infection confer enhanced susceptibility to *C. albicans*, we monitored mice over time after in vivo infection. Strikingly, and consistent with the above data, *Trim62*$^{-/-}$ mice were more susceptible to in vivo *C. albicans* infection, such that they showed 100% mortality by day 15 after infection (Figure 6D).

Given the association between this pathway and IBD, we also assessed *Trim62*$^{-/-}$ mice in the dextran sulfate sodium (DSS) model of intestinal inflammation. As in previously published studies in *Card9*$^{-/-}$ mice, compared to wild-type mice treated with DSS, *Trim62*$^{-/-}$ mice showed increased weight loss, greater inflammation, and impaired cytokine responses (Figures S6E–S6G). Taken together, these results demonstrate that TRIM62 is important for immunity in in vivo models of *C. albicans* infection and DSS-induced colitis.

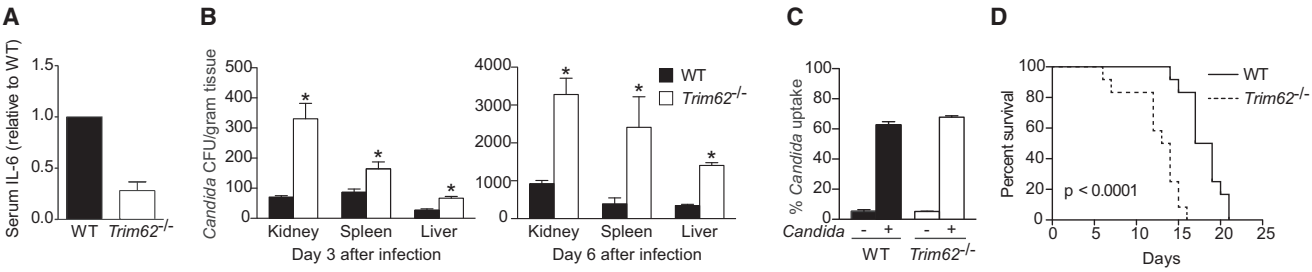

Figure 6. TRIM62 Regulates Immune Responses and Susceptibility to *C. albicans* Infection In Vivo

(A) Wild-type (WT) and *Trim62*$^{-/-}$ mice were injected i.v. with heat-killed *C. albicans*, and serum IL-6 amounts were quantified 4 hr later by ELISA (n = 5). Bars display IL-6 relative to WT amounts.

(B) WT and *Trim62*$^{-/-}$ mice were injected with *C. albicans*, and fungal loads in the kidney, spleen, and liver were assessed 3 and 6 days after infection.

(C) WT and *Trim62*$^{-/-}$ BMDMs were incubated with pHrodo-labeled *C. albicans*, and phagocytosed *C. albicans* was quantified by intracellular fluorescence via flow cytometry.

(D) A survival curve shows the percentage of survival over time in WT and *Trim62*$^{-/-}$ mice infected with *C. albicans*. Bars represent means ± SD. *p < 0.05. See also Figure S6.

DISCUSSION

CARD9 coding mutations are associated with multiple immune-related diseases, underscoring the physiologic importance of CARD9 signaling in immunity. In the current study, we used a *CARD9* allele strongly protective against IBD as an entry point to uncovering basic insights into the biology of CARD9 regulation, as well as a potential mechanism for the protective effect of the Δ11 variant. Through systematic pathway mapping, we found a CARD9 C-terminal interacting partner that regulates CARD9 function in a ligand-specific manner; this interactor (TRIM62), which does not interact with the protective variant of CARD9, acts as an E3 ubiquitin ligase to activate CARD9 function. Given our findings that TRIM62 acts as a restriction factor for fungal infections, our results expand the list of E3 ligases that function as restriction factors and extend the range of pathogens implicated in TRIM family signaling. The TRIM family of proteins expanded relatively recently in evolution (Ozato et al., 2008) and play important roles in the crosstalk between the innate and adaptive immune systems (Rajsbaum et al., 2014a). The majority of studies of TRIM proteins have focused on their roles as antiviral restriction factors (Ozato et al., 2008), and recent screens have reported that mRNA and localization of most known TRIM proteins are altered during viral infection (Uchil et al., 2013; Versteeg et al., 2013). Extending these studies, a recent report identified that TRIM5 is a regulator of autophagy and acts as a restriction factor against HIV-1 (Mandell et al., 2014). TRIM family members largely function in negative regulatory circuits, as was recently demonstrated for TRIM9, a negative regulator of NF-κB pro-inflammatory cytokine signaling (Shi et al., 2014). An increasing number of TRIM proteins have also been described as enhancers of innate immune pathways, as in the case for TRIM44, which stabilizes MAVS to enhance signaling (Yang et al., 2013). TRIM proteins mediate several types of ubiquitin linkages, and most studies focus on K48- and K63-based linkages and their respective roles in degradation and stabilization of protein complexes (Davis and Gack, 2015; Flannick et al., 2014; Gack et al., 2007; Rajsbaum et al., 2014b; Tsuchida et al., 2010; Zhao et al., 2012), although K27-linked ubiquitination has been reported for TRIM23 (Arimoto et al., 2010). Our findings of TRIM62-mediated K27-linked ubiquitination of CARD9 suggest that this type of linkage promotes an important mechanism for protein activation, although notably the K125R alteration does not affect colocalization of CARD9 and BCL10.

To date, all clinically reported homozygous or compound-heterozygous carriers with either no CARD9 expression or CARD9 loss of function are more susceptible to fungal infection (Drewniak et al., 2013; Gavino et al., 2014; Gazendam et al., 2014; Glocker et al., 2009; Grumach et al., 2015; Herbst et al., 2015; Jachiet et al., 2015; Lanternier et al., 2015a; Lanternier et al., 2015b; Lanternier et al., 2013; Wang et al., 2014). Our results from *Trim62*$^{-/-}$ mice suggest that TRIM62-mediated regulation of CARD9 activation is critical in the context of fungal infection. These data complement previous studies reporting critical roles for CARD9 and PKCδ during *C. albicans* infection and suggest that TRIM62 is a novel member of this pathway and is important for anti-fungal immunity (Gross et al., 2006; Strasser et al., 2012). Furthermore, we found that *Trim62*$^{-/-}$ mice, similar to *Card9*$^{-/-}$ mice, are more susceptible to DSS colitis, underscoring the importance of this pathway in intestinal homeostasis and fortifying previous reports on the relationship between fungi and IBD (Chehoud et al., 2015; Richard et al., 2015; Romani, 2011).

Next-generation sequencing has identified both a common predisposing allele and rare protective splice variant in *CARD9* (Rivas et al., 2011). The presence of both common and rare risk variants in a single gene has now been increasingly observed in multiple studies, advancing the concept that when multiple common and rare variants are discovered, the resulting allelic series can serve to anchor a dose-response relationship between gene and disease. For example, the connection between rare genetic variants and therapeutic advances has been well demonstrated by *PCSK9* in modulating amounts of low-density lipoprotein cholesterol, where protective variation can be therapeutically mimicked (Cohen et al., 2006), and a recent finding of *SLC30A8* loss-of-function mutations that protect against type 2 diabetes (Flannick et al., 2014). Our findings demonstrate that the protective CARD9 variant does not undergo ubiquitination by TRIM62, and we propose that the protective effect of

the C-terminal truncation might be mediated by loss of TRIM62 interaction and thereby limit proinflammatory cytokine responses. Given that TRIM62-dependent ubiquitination and subsequent activation of CARD9 might be targetable, these findings suggest a model in which a naturally occurring protective allele might be used as a guide for rational design of therapeutics. Indeed, evolution has "validated" this approach as a safe and effective strategy for decreasing the likelihood of developing IBD.

EXPERIMENTAL PROCEDURES

Plasmids

For lentiviral vectors, FLAG-StrepII fusion human CARD9 variants were constructed by PCR-based subcloning of CARD9 coding sequences into a lentivirus-based CSGW vector backbone (gift from Christian Münz, University of Zurich). For other CARD9 constructs, CARD9 was cloned into either a pCMV vector (see section "CARD9 Variant Cloning" in the Supplemental Experimental Procedures) or pcDNA4/TO-FLAG-StrepII. Ubiquitin cDNA was kindly provided by Dr. M. Scheffner (University of Konstanz, Germany). All other genes were originally obtained from either OpenBiosystems or Origene and subcloned into indicated tagged vectors by PCR. Wild-type and altered ubiquitin, SUMO1, SUMO2, SUMO3, and ISG15 were subcloned into pCMV-3xMyc. pCMV-3xHA and pCMV-3xMyc were derived from pCMV-Myc (Clontech). TRIM62 constructs were subcloned into either pCMV-3xHA or pcDNA4/TO-V5. pcDNA4/TO-FLAG-StrepII and pcDNA4/TO-V5 were derived from pcDNA4/TO (Invitrogen). FLAG-StrepII, HA, and Myc are all N-terminal tags. All cDNAs were confirmed by DNA sequencing.

Chemical Reagents

Depleted zymosan was purchased from Invivogen. Trehalose 6,6'-dimycolate (TDM) was obtained from Enzo Life Sciences. TDM was dissolved in 1 mg/ml chloroform, methanol, and water at a 90:10:1 ratio and further diluted with isopropanol. LPS was purchased from Sigma or Invivogen.

Cell Culture and Lentiviral Production

HEK293T and HeLa cells were maintained at 37°C and 5% CO_2 in DMEM supplemented with 10% fetal calf serum and 15 μg/ml gentamycin sulfate. THP-1 cells were maintained at 37°C and 5% CO_2 in RPMI1640 supplemented with 10% fetal calf serum, 5×10^{-4}M beta-mercaptoethanol, and 15 μg/ml gentamycin sulfate. For preparing lentivirus for infection, protocols from the Broad Institute's RNAi Consortium shRNA Library were used (http://www.broadinstitute.org/rnai/trc/lib). The Lentivirus qPCR Titer Kit (Applied Biological Materials) was used for lentiviral titration. pSIV3$^+$ plasmid for generating Vpx-VLP was a gift from Dr. Andrea Cimarelli (École Normale Supérieure de Lyon, France) (Berger et al., 2011).

Trim62$^{-/-}$ Mouse Strain

Trim62-heterozygous mice on the 129/SvEv genetic background were purchased from Taconic (catalog no. TF2743). *Trim62*-heterozygous mice, derived from an F1 generation of the *Trim62*-heterozygous mice from Taconic and C57BL/6 mice with wild-type *Trim62*, were bred for generating wild-type or *Trim62*$^{-/-}$ littermates. The targeted locus is located at the junction of the first exon and first intron of *Trim62*, resulting in deletion of a portion of the exon 1 coding region and intron 1 of *Trim62*. See also Figure S6. *Trim62*$^{-/-}$ mice are viable and born at Mendelian ratios.

Preparation of Heat-Killed *C. albicans*

C. albicans strain SC5314 (ATCC MYA-2876) was obtained from Eleftherios Mylonakis (Massachusetts General Hospital, Boston). *C. albicans* were harvested from an overnight culture in YPD medium (Y1375, Sigma) at 30°C. *C. albicans* were washed with PBS twice and resuspended in PBS at 2×10^8/ml. Resuspended *C. albicans* were then incubated for 2 hr at 68°C and cooled on ice. Heat-killed cell death was verified by cell plating on YPD agar plates.

In Vivo Injection of Heat-Killed *C. albicans*

1×10^7 heat-killed *C. albicans* in PBS were injected intravenously (i.v.). After 4 hr, serum was harvested, and IL-6 amounts were determined via ELISA.

Ex Vivo Splenic DC Stimulations and Intracellular Phosphoprotein Staining

CD11c$^+$ cells were positively selected from the spleen with MACS technology according to the manufacturer's (Miltenyi Biotec) protocol. 1×10^6 cells were resuspended in complete RPMI (10% fetal bovine serum and 15 μg/ml gentamicin) and incubated for 10 min at 37°C with 5% CO_2 in one of three conditions: (1) no stimulation, (2) 100 ng/ml LPS stimulation, or (3) 1×10^6 heat-killed *C. albicans* stimulation. Cells were immediately fixed with BD Cytofix Fixation Buffer and permeabilized with BD Phosflow Permeabilization Buffer 3 according to the manufacturer's (BD Biosciences) protocol. After 20 min of Fc block on ice, cells were stained as indicated with the following antibodies: CD11c-PECy7 (BD Biosciences), phospho-ERK1/2-PE (BD Biosciences), phospho-IκBα (Cell Signaling Technologies), and donkey anti-rabbit IgG DyLight 488 (BioLegend). Cells were acquired on the BD FACSVerse (BD Biosciences) and analyzed with FlowJo Software.

C. albicans for In Vivo Infection

C. albicans (strain ATCC 90028) were grown on yeast-peptone-dextrose agar (Difco) at 30°C. For each infection, a fresh culture of *C. albicans* was started from −80°C stocks. For experiments, a fresh colony was isolated from an agar plate and grown in YPD media for 24 hr at 30°C. Prior to inoculation, yeast cells were washed three times in PBS, counted, and adjusted to the appropriate concentration.

Viable *C. albicans* Counts

Mice were infected i.v. with 10^5 *C. albicans* and sacrificed on days 3 and 6 after infection. CFUs of *C. albicans* in the homogenized kidney, spleen, and liver were determined by plate counts. Data are expressed as CFU per mg of tissue.

Mice

Card9$^{-/-}$ mice have been previously described (Hara et al., 2007). Mice were maintained in specific-pathogen-free facilities at Massachusetts General Hospital. All animal studies were conducted under protocols approved by the Institutional Animal Care and Use Committee (IACUC) at Massachusetts General Hospital.

Statistical Analysis

Unpaired two-tailed Student's t tests were used for comparisons for ELISA. All statistical comparisons were made between multiple independent experiments performed in parallel.

SUPPLEMENTAL INFORMATION

Supplemental Information includes Supplemental Experimental Procedures and six figures and can be found with this article online at http://dx.doi.org/10.1016/j.immuni.2015.10.005.

AUTHOR CONTRIBUTIONS

R.J.X. and Z.C. conceived the project. Z.C., K.L.C., R.J.H., J.S.R., E.S.L., Z.G.R.-O., A.N., A.G., S.-C.C., and T.K.M. performed experiments, and H.H. analyzed Immunochip data. R.J.X., M.J.D., and T.K.M. supervised the project. A.F.S., J.D.R., C.W., and M.G.N. provided intellectual contributions throughout the project. R.J.X., N.B.N., and Z.C. wrote the manuscript. All authors discussed the results and commented on the manuscript.

ACKNOWLEDGMENTS

We thank Drs. Hiromitsu Hara (Saga Medical School, Japan) for providing *Card9*$^{-/-}$ mice (Hara et al., 2007), Kara Lassen for guidance with manuscript preparation, and Petric Kuballa, Jakob Begun, and David Fei for assistance with experiments. This work was supported by funding from the Helmsley Trust and NIH grants DK097485, DK062432, and DK086502 to R.J.X. M.G.N. was supported by an ERC Consolidator Grant (no. 310372). T.K.M.

was supported by NIH grant AI084884. Z.G.R.-O. was supported by NIH grant AR066716.

Received: May 12, 2014
Revised: April 8, 2015
Accepted: July 24, 2015
Published: October 20, 2015

REFERENCES

Abdullah, Z., Schlee, M., Roth, S., Mraheil, M.A., Barchet, W., Böttcher, J., Hain, T., Geiger, S., Hayakawa, Y., Fritz, J.H., et al. (2012). RIG-I detects infection with live Listeria by sensing secreted bacterial nucleic acids. EMBO J. *31*, 4153–4164.

Arimoto, K., Funami, K., Saeki, Y., Tanaka, K., Okawa, K., Takeuchi, O., Akira, S., Murakami, Y., and Shimotohno, K. (2010). Polyubiquitin conjugation to NEMO by triparite motif protein 23 (TRIM23) is critical in antiviral defense. Proc. Natl. Acad. Sci. USA *107*, 15856–15861.

Beaudoin, M., Goyette, P., Boucher, G., Lo, K.S., Rivas, M.A., Stevens, C., Alikashani, A., Ladouceur, M., Ellinghaus, D., Törkvist, L., et al.; Quebec IBD Genetics Consortium; NIDDK IBD Genetics Consortium; International IBD Genetics Consortium (2013). Deep resequencing of GWAS loci identifies rare variants in CARD9, IL23R and RNF186 that are associated with ulcerative colitis. PLoS Genet. *9*, e1003723.

Berger, G., Durand, S., Goujon, C., Nguyen, X.N., Cordeil, S., Darlix, J.L., and Cimarelli, A. (2011). A simple, versatile and efficient method to genetically modify human monocyte-derived dendritic cells with HIV-1-derived lentiviral vectors. Nat. Protoc. *6*, 806–816.

Blasi, E., Mathieson, B.J., Varesio, L., Cleveland, J.L., Borchert, P.A., and Rapp, U.R. (1985). Selective immortalization of murine macrophages from fresh bone marrow by a raf/myc recombinant murine retrovirus. Nature *318*, 667–670.

Campbell, E.M., Dodding, M.P., Yap, M.W., Wu, X., Gallois-Montbrun, S., Malim, M.H., Stoye, J.P., and Hope, T.J. (2007). TRIM5 alpha cytoplasmic bodies are highly dynamic structures. Mol. Biol. Cell *18*, 2102–2111.

Chehoud, C., Albenberg, L.G., Judge, C., Hoffmann, C., Grunberg, S., Bittinger, K., Baldassano, R.N., Lewis, J.D., Bushman, F.D., and Wu, G.D. (2015). Fungal Signature in the Gut Microbiota of Pediatric Patients With Inflammatory Bowel Disease. Inflamm. Bowel Dis. *21*, 1948–1956.

Chu, Y., and Yang, X. (2011). SUMO E3 ligase activity of TRIM proteins. Oncogene *30*, 1108–1116.

Cohen, J.C., Boerwinkle, E., Mosley, T.H., Jr., and Hobbs, H.H. (2006). Sequence variations in PCSK9, low LDL, and protection against coronary heart disease. N. Engl. J. Med. *354*, 1264–1272.

Davis, M.E., and Gack, M.U. (2015). Ubiquitination in the antiviral immune response. Virology *479–480*, 52–65.

Deshaies, R.J., and Joazeiro, C.A. (2009). RING domain E3 ubiquitin ligases. Annu. Rev. Biochem. *78*, 399–434.

Drewniak, A., Gazendam, R.P., Tool, A.T., van Houdt, M., Jansen, M.H., van Hamme, J.L., van Leeuwen, E.M., Roos, D., Scalais, E., de Beaufort, C., et al. (2013). Invasive fungal infection and impaired neutrophil killing in human CARD9 deficiency. Blood *121*, 2385–2392.

Drummond, R.A., Saijo, S., Iwakura, Y., and Brown, G.D. (2011). The role of Syk/CARD9 coupled C-type lectins in antifungal immunity. Eur. J. Immunol. *41*, 276–281.

Flannick, J., Thorleifsson, G., Beer, N.L., Jacobs, S.B., Grarup, N., Burtt, N.P., Mahajan, A., Fuchsberger, C., Atzmon, G., Benediktsson, R., et al.; Go-T2D Consortium; T2D-GENES Consortium (2014). Loss-of-function mutations in SLC30A8 protect against type 2 diabetes. Nat. Genet. *46*, 357–363.

Franke, A., McGovern, D.P., Barrett, J.C., Wang, K., Radford-Smith, G.L., Ahmad, T., Lees, C.W., Balschun, T., Lee, J., Roberts, R., et al. (2010). Genome-wide meta-analysis increases to 71 the number of confirmed Crohn's disease susceptibility loci. Nat. Genet. *42*, 1118–1125.

Fuchs, T., Saunders-Pullman, R., Masuho, I., Luciano, M.S., Raymond, D., Factor, S., Lang, A.E., Liang, T.W., Trosch, R.M., White, S., et al. (2013). Mutations in GNAL cause primary torsion dystonia. Nat. Genet. *45*, 88–92.

Gack, M.U., Shin, Y.C., Joo, C.H., Urano, T., Liang, C., Sun, L., Takeuchi, O., Akira, S., Chen, Z., Inoue, S., and Jung, J.U. (2007). TRIM25 RING-finger E3 ubiquitin ligase is essential for RIG-I-mediated antiviral activity. Nature *446*, 916–920.

Gavino, C., Cotter, A., Lichtenstein, D., Lejtenyi, D., Fortin, C., Legault, C., Alirezaie, N., Majewski, J., Sheppard, D.C., Behr, M.A., et al. (2014). CARD9 deficiency and spontaneous central nervous system candidiasis: complete clinical remission with GM-CSF therapy. Clin. Infect. Dis. *59*, 81–84.

Gazendam, R.P., van Hamme, J.L., Tool, A.T., van Houdt, M., Verkuijlen, P.J., Herbst, M., Liese, J.G., van de Veerdonk, F.L., Roos, D., van den Berg, T.K., and Kuijpers, T.W. (2014). Two independent killing mechanisms of Candida albicans by human neutrophils: evidence from innate immunity defects. Blood *124*, 590–597.

Glocker, E.O., Hennigs, A., Nabavi, M., Schäffer, A.A., Woellner, C., Salzer, U., Pfeifer, D., Veelken, H., Warnatz, K., Tahami, F., et al. (2009). A homozygous CARD9 mutation in a family with susceptibility to fungal infections. N. Engl. J. Med. *361*, 1727–1735.

Goodridge, H.S., Shimada, T., Wolf, A.J., Hsu, Y.M., Becker, C.A., Lin, X., and Underhill, D.M. (2009). Differential use of CARD9 by dectin-1 in macrophages and dendritic cells. J. Immunol. *182*, 1146–1154.

Gross, O., Gewies, A., Finger, K., Schäfer, M., Sparwasser, T., Peschel, C., Förster, I., and Ruland, J. (2006). Card9 controls a non-TLR signalling pathway for innate anti-fungal immunity. Nature *442*, 651–656.

Grumach, A.S., de Queiroz-Telles, F., Migaud, M., Lanternier, F., Filho, N.R., Palma, S.M., Constantino-Silva, R.N., Casanova, J.L., and Puel, A. (2015). A homozygous CARD9 mutation in a Brazilian patient with deep dermatophytosis. J. Clin. Immunol. *35*, 486–490.

Hara, H., and Saito, T. (2009). CARD9 versus CARMA1 in innate and adaptive immunity. Trends Immunol. *30*, 234–242.

Hara, H., Ishihara, C., Takeuchi, A., Imanishi, T., Xue, L., Morris, S.W., Inui, M., Takai, T., Shibuya, A., Saijo, S., et al. (2007). The adaptor protein CARD9 is essential for the activation of myeloid cells through ITAM-associated and Toll-like receptors. Nat. Immunol. *8*, 619–629.

Herbst, M., Gazendam, R., Reimnitz, D., Sawalle-Belohradsky, J., Groll, A., Schlegel, P.G., Belohradsky, B., Renner, E., Klepper, J., Grimbacher, B., et al. (2015). Chronic Candida albicans Meningitis in a 4-Year-Old Girl with a Homozygous Mutation in the CARD9 Gene (Q295X). Pediatr. Infect. Dis. J. *34*, 999–1002.

Ishikawa, E., Ishikawa, T., Morita, Y.S., Toyonaga, K., Yamada, H., Takeuchi, O., Kinoshita, T., Akira, S., Yoshikai, Y., and Yamasaki, S. (2009). Direct recognition of the mycobacterial glycolipid, trehalose dimycolate, by C-type lectin Mincle. J. Exp. Med. *206*, 2879–2888.

Jachiet, M., Lanternier, F., Rybojad, M., Bagot, M., Ibrahim, L., Casanova, J.L., Puel, A., and Bouaziz, J.D. (2015). Posaconazole treatment of extensive skin and nail dermatophytosis due to autosomal recessive deficiency of CARD9. JAMA Dermatol. *151*, 192–194.

Janse, M., Lamberts, L.E., Franke, L., Raychaudhuri, S., Ellinghaus, E., Muri Boberg, K., Melum, E., Folseraas, T., Schrumpf, E., Bergquist, A., et al. (2011). Three ulcerative colitis susceptibility loci are associated with primary sclerosing cholangitis and indicate a role for IL2, REL, and CARD9. Hepatology *53*, 1977–1985.

Jia, X.M., Tang, B., Zhu, L.L., Liu, Y.H., Zhao, X.Q., Gorjestani, S., Hsu, Y.M., Yang, L., Guan, J.H., Xu, G.T., and Lin, X. (2014). CARD9 mediates Dectin-1-induced ERK activation by linking Ras-GRF1 to H-Ras for antifungal immunity. J. Exp. Med. *211*, 2307–2321.

Jostins, L., Ripke, S., Weersma, R.K., Duerr, R.H., McGovern, D.P., Hui, K.Y., Lee, J.C., Schumm, L.P., Sharma, Y., Anderson, C.A., et al.; International IBD Genetics Consortium (IIBDGC) (2012). Host-microbe interactions have shaped the genetic architecture of inflammatory bowel disease. Nature *491*, 119–124.

Kiryluk, K., Li, Y., Scolari, F., Sanna-Cherchi, S., Choi, M., Verbitsky, M., Fasel, D., Lata, S., Prakash, S., Shapiro, S., et al. (2014). Discovery of new risk loci for

IgA nephropathy implicates genes involved in immunity against intestinal pathogens. Nat. Genet. *46*, 1187–1196.

Lanternier, F., Pathan, S., Vincent, Q.B., Liu, L., Cypowyj, S., Prando, C., Migaud, M., Taibi, L., Ammar-Khodja, A., Boudghene Stambouli, O., et al. (2013). Deep dermatophytosis and inherited CARD9 deficiency. N. Engl. J. Med. *369*, 1704–1714.

Lanternier, F., Barbati, E., Meinzer, U., Liu, L., Pedergnana, V., Migaud, M., Héritier, S., Chomton, M., Frémond, M.L., Gonzales, E., et al. (2015a). Inherited CARD9 deficiency in 2 unrelated patients with invasive Exophiala infection. J. Infect. Dis. *211*, 1241–1250.

Lanternier, F., Mahdaviani, S.A., Barbati, E., Chaussade, H., Koumar, Y., Levy, R., Denis, B., Brunel, A.S., Martin, S., Loop, M., et al. (2015b). Inherited CARD9 deficiency in otherwise healthy children and adults with Candida species-induced meningoencephalitis, colitis, or both. J. Allergy Clin. Immunol. *135*, 1558–68.e2.

LeibundGut-Landmann, S., Gross, O., Robinson, M.J., Osorio, F., Slack, E.C., Tsoni, S.V., Schweighoffer, E., Tybulewicz, V., Brown, G.D., Ruland, J., and Reis e Sousa, C. (2007). Syk- and CARD9-dependent coupling of innate immunity to the induction of T helper cells that produce interleukin 17. Nat. Immunol. *8*, 630–638.

Mandell, M.A., Kimura, T., Jain, A., Johansen, T., and Deretic, V. (2014). TRIM proteins regulate autophagy: TRIM5 is a selective autophagy receptor mediating HIV-1 restriction. Autophagy *10*, 2387–2388.

Marakalala, M.J., Graham, L.M., and Brown, G.D. (2010). The role of Syk/CARD9-coupled C-type lectin receptors in immunity to Mycobacterium tuberculosis infections. Clin. Dev. Immunol. *2010*, 567571.

Marín, I. (2012). Origin and diversification of TRIM ubiquitin ligases. PLoS ONE *7*, e50030.

McGovern, D.P., Gardet, A., Törkvist, L., Goyette, P., Essers, J., Taylor, K.D., Neale, B.M., Ong, R.T., Lagacé, C., Li, C., et al.; NIDDK IBD Genetics Consortium (2010). Genome-wide association identifies multiple ulcerative colitis susceptibility loci. Nat. Genet. *42*, 332–337.

McNab, F.W., Rajsbaum, R., Stoye, J.P., and O'Garra, A. (2011). Tripartite-motif proteins and innate immune regulation. Curr. Opin. Immunol. *23*, 46–56.

Miyake, Y., Toyonaga, K., Mori, D., Kakuta, S., Hoshino, Y., Oyamada, A., Yamada, H., Ono, K., Suyama, M., Iwakura, Y., et al. (2013). C-type lectin MCL is an FcRγ-coupled receptor that mediates the adjuvanticity of mycobacterial cord factor. Immunity *38*, 1050–1062.

Ozato, K., Shin, D.M., Chang, T.H., and Morse, H.C., 3rd (2008). TRIM family proteins and their emerging roles in innate immunity. Nat. Rev. Immunol. *8*, 849–860.

Papa, A., Wan, L., Bonora, M., Salmena, L., Song, M.S., Hobbs, R.M., Lunardi, A., Webster, K., Ng, C., Newton, R.H., et al. (2014). Cancer-associated PTEN mutants act in a dominant-negative manner to suppress PTEN protein function. Cell *157*, 595–610.

Poeck, H., Bscheider, M., Gross, O., Finger, K., Roth, S., Rebsamen, M., Hannesschläger, N., Schlee, M., Rothenfusser, S., Barchet, W., et al. (2010). Recognition of RNA virus by RIG-I results in activation of CARD9 and inflammasome signaling for interleukin 1 beta production. Nat. Immunol. *11*, 63–69.

Pointon, J.J., Harvey, D., Karaderi, T., Appleton, L.H., Farrar, C., Stone, M.A., Sturrock, R.D., Brown, M.A., and Wordsworth, B.P. (2010). Elucidating the chromosome 9 association with AS; CARD9 is a candidate gene. Genes Immun. *11*, 490–496.

Rajsbaum, R., García-Sastre, A., and Versteeg, G.A. (2014a). TRIMmunity: the roles of the TRIM E3-ubiquitin ligase family in innate antiviral immunity. J. Mol. Biol. *426*, 1265–1284.

Rajsbaum, R., Versteeg, G.A., Schmid, S., Maestre, A.M., Belicha-Villanueva, A., Martínez-Romero, C., Patel, J.R., Morrison, J., Pisanelli, G., Miorin, L., et al. (2014b). Unanchored K48-linked polyubiquitin synthesized by the E3-ubiquitin ligase TRIM6 stimulates the interferon-IKKε kinase-mediated antiviral response. Immunity *40*, 880–895.

Reymond, A., Meroni, G., Fantozzi, A., Merla, G., Cairo, S., Luzi, L., Riganelli, D., Zanaria, E., Messali, S., Cainarca, S., et al. (2001). The tripartite motif family identifies cell compartments. EMBO J. *20*, 2140–2151.

Richard, M.L., Lamas, B., Liguori, G., Hoffmann, T.W., and Sokol, H. (2015). Gut fungal microbiota: the Yin and Yang of inflammatory bowel disease. Inflamm. Bowel Dis. *21*, 656–665.

Rieber, N., Singh, A., Öz, H., Carevic, M., Bouzani, M., Amich, J., Ost, M., Ye, Z., Ballbach, M., Schäfer, I., et al. (2015). Pathogenic fungi regulate immunity by inducing neutrophilic myeloid-derived suppressor cells. Cell Host Microbe *17*, 507–514.

Rivas, M.A., Beaudoin, M., Gardet, A., Stevens, C., Sharma, Y., Zhang, C.K., Boucher, G., Ripke, S., Ellinghaus, D., Burtt, N., et al.; National Institute of Diabetes and Digestive Kidney Diseases Inflammatory Bowel Disease Genetics Consortium (NIDDK IBDGC); United Kingdom Inflammatory Bowel Disease Genetics Consortium; International Inflammatory Bowel Disease Genetics Consortium (2011). Deep resequencing of GWAS loci identifies independent rare variants associated with inflammatory bowel disease. Nat. Genet. *43*, 1066–1073.

Robinson, M.J., Osorio, F., Rosas, M., Freitas, R.P., Schweighoffer, E., Gross, O., Verbeek, J.S., Ruland, J., Tybulewicz, V., Brown, G.D., et al. (2009). Dectin-2 is a Syk-coupled pattern recognition receptor crucial for Th17 responses to fungal infection. J. Exp. Med. *206*, 2037–2051.

Romani, L. (2011). Immunity to fungal infections. Nat. Rev. Immunol. *11*, 275–288.

Roth, S., and Ruland, J. (2013). Caspase recruitment domain-containing protein 9 signaling in innate immunity and inflammation. Trends Immunol. *34*, 243–250.

Roth, S., Rottach, A., Lotz-Havla, A.S., Laux, V., Muschaweckh, A., Gersting, S.W., Muntau, A.C., Hopfner, K.P., Jin, L., Vanness, K., et al. (2014). Rad50-CARD9 interactions link cytosolic DNA sensing to IL-1β production. Nat. Immunol. *15*, 538–545.

Saijo, S., Ikeda, S., Yamabe, K., Kakuta, S., Ishigame, H., Akitsu, A., Fujikado, N., Kusaka, T., Kubo, S., Chung, S.H., et al. (2010). Dectin-2 recognition of alpha-mannans and induction of Th17 cell differentiation is essential for host defense against Candida albicans. Immunity *32*, 681–691.

Schoenen, H., Bodendorfer, B., Hitchens, K., Manzanero, S., Werninghaus, K., Nimmerjahn, F., Agger, E.M., Stenger, S., Andersen, P., Ruland, J., et al. (2010). Cutting edge: Mincle is essential for recognition and adjuvanticity of the mycobacterial cord factor and its synthetic analog trehalose-dibehenate. J. Immunol. *184*, 2756–2760.

Shi, M., Cho, H., Inn, K.S., Yang, A., Zhao, Z., Liang, Q., Versteeg, G.A., Amini-Bavil-Olyaee, S., Wong, L.Y., Zlokovic, B.V., et al. (2014). Negative regulation of NF-κB activity by brain-specific TRIpartite Motif protein 9. Nat. Commun. *5*, 4820.

Sokol, H., Conway, K.L., Zhang, M., Choi, M., Morin, B., Cao, Z., Villablanca, E.J., Li, C., Wijmenga, C., Yun, S.H., et al. (2013). Card9 mediates intestinal epithelial cell restitution, T-helper 17 responses, and control of bacterial infection in mice. Gastroenterology *145*, 591–601.e3.

Strasser, D., Neumann, K., Bergmann, H., Marakalala, M.J., Guler, R., Rojowska, A., Hopfner, K.P., Brombacher, F., Urlaub, H., Baier, G., et al. (2012). Syk kinase-coupled C-type lectin receptors engage protein kinase C-σ to elicit Card9 adaptor-mediated innate immunity. Immunity *36*, 32–42.

Tsuchida, T., Zou, J., Saitoh, T., Kumar, H., Abe, T., Matsuura, Y., Kawai, T., and Akira, S. (2010). The ubiquitin ligase TRIM56 regulates innate immune responses to intracellular double-stranded DNA. Immunity *33*, 765–776.

Uchil, P.D., Hinz, A., Siegel, S., Coenen-Stass, A., Pertel, T., Luban, J., and Mothes, W. (2013). TRIM protein-mediated regulation of inflammatory and innate immune signaling and its association with antiretroviral activity. J. Virol. *87*, 257–272.

Versteeg, G.A., Rajsbaum, R., Sánchez-Aparicio, M.T., Maestre, A.M., Valdiviezo, J., Shi, M., Inn, K.S., Fernandez-Sesma, A., Jung, J., and García-Sastre, A. (2013). The E3-ligase TRIM family of proteins regulates signaling pathways triggered by innate immune pattern-recognition receptors. Immunity *38*, 384–398.

Wang, X., Wang, W., Lin, Z., Wang, X., Li, T., Yu, J., Liu, W., Tong, Z., Xu, Y., Zhang, J., et al. (2014). CARD9 mutations linked to subcutaneous phaeohyphomycosis and TH17 cell deficiencies. J. Allergy Clin. Immunol. *133*, 905–8.e3.

Werninghaus, K., Babiak, A., Gross, O., Hölscher, C., Dietrich, H., Agger, E.M., Mages, J., Mocsai, A., Schoenen, H., Finger, K., et al. (2009). Adjuvanticity of a synthetic cord factor analogue for subunit Mycobacterium tuberculosis vaccination requires FcRgamma-Syk-Card9-dependent innate immune activation. J. Exp. Med. *206*, 89–97.

Yang, C.S., Rodgers, M., Min, C.K., Lee, J.S., Kingeter, L., Lee, J.Y., Jong, A., Kramnik, I., Lin, X., and Jung, J.U. (2012). The autophagy regulator Rubicon is a feedback inhibitor of CARD9-mediated host innate immunity. Cell Host Microbe *11*, 277–289.

Yang, B., Wang, J., Wang, Y., Zhou, H., Wu, X., Tian, Z., and Sun, B. (2013). Novel function of Trim44 promotes an antiviral response by stabilizing VISA. J. Immunol. *190*, 3613–3619.

Zhang, Z., Bao, M., Lu, N., Weng, L., Yuan, B., and Liu, Y.J. (2013). The E3 ubiquitin ligase TRIM21 negatively regulates the innate immune response to intracellular double-stranded DNA. Nat. Immunol. *14*, 172–178.

Zhao, W., Wang, L., Zhang, M., Wang, P., Yuan, C., Qi, J., Meng, H., and Gao, C. (2012). Tripartite motif-containing protein 38 negatively regulates TLR3/4- and RIG-I-mediated IFN-β production and antiviral response by targeting NAP1. J. Immunol. *188*, 5311–5318.

Zhernakova, A., Festen, E.M., Franke, L., Trynka, G., van Diemen, C.C., Monsuur, A.J., Bevova, M., Nijmeijer, R.M., van 't Slot, R., Heijmans, R., et al. (2008). Genetic analysis of innate immunity in Crohn's disease and ulcerative colitis identifies two susceptibility loci harboring CARD9 and IL18RAP. Am. J. Hum. Genet. *82*, 1202–1210.